

PREPARATION AND CHARACTERIZATION OF POLYMER INCLUSION MEMBRANES BASED ON BIODEGRADABLE CELLULOSE/ALGERIAN CLAY FOR HEAVY METALS REMOVAL FROM WASTEWATER

AMINA AOUES,^{*,**} OUARDA MERDOUD,^{**,***} MOHAMED OUALID BOULAKRADECHE,^{**} OMAR AROUS^{**} and DJAMAL ABDESSEMED^{*}

^{*}Laboratory of Sciences and Industrial Processes Engineering, Department of the Environment Engineering, USTHB, PO Box 32, El Alia, Bab Ezzouar, 16111, Algiers, Algeria

^{**}Laboratory of Hydrometallurgy and Inorganic Molecular Chemistry (LHCIM), Faculty of Chemistry, USTHB, PO Box 32, El Alia, Bab Ezzouar, 16111, Algiers, Algeria

^{***}Center of Research in Physical and Chemical Analysis (CRAPC), Bousmail, Tipaza, Algeria

✉ Corresponding author: O. Arous, omararous@yahoo.fr

Received April 19, 2024

Separation membranes have gained attention as promising options for water and wastewater treatment due to their financial sustainability, and eco-friendliness. However, practical challenges have limited their application in water separation. To overcome these limitations, inorganic-organic hybrid membranes have been developed in this study. The present work deals with two attractive aspects: (i) economical, through the valorization of a local clay (Algerian kaolin), and (ii) environmental, which is based on the membrane selectivity for metal ions. The principal objective of this work is the development of enhanced nanocomposite membranes. It is achieved with low costs, based on cellulose triacetate (CTA) as a polymeric matrix modified by the addition of a lamellar filler, *i.e.* yellow clay obtained from Jijel, located in the east of Algeria, and plasticized by dioctyl phthalate (DOP). A further objective of this paper was the treatment of wastewater polluted by lead (Pb²⁺) and cadmium (Cd²⁺). The prepared membranes were characterized by various characterization techniques, including scanning electron microscopy (SEM), Fourier-transform infrared (FTIR) spectroscopy and thermogravimetric analysis (TGA).

All synthesized membranes had an amorphous structure, with homogeneous pore morphology and distribution. Moreover, the presence of nanocomposite clay showed effective integration into the membrane matrix and led to a significant improvement in thermal resistance. These membranes were applied to treat a synthetic aqueous solution contaminated with heavy metals, namely Pb²⁺ and Cd²⁺. The results revealed a rejection rate higher than 50%, suggesting the potential effectiveness of a stable and environmentally sustainable polymer inclusion membrane system for water purification.

Keywords: hybrid membrane, Algerian kaolin, heavy metal, cellulose triacetate

INTRODUCTION

Protecting the environment from various types of pollution, linked mainly to the release of toxic heavy metals, requires the use of new, clean, efficient, sustainable and less expensive technologies. Water pollution control has become a priority even for developing countries. Currently, environmental research is focused on classic separation methods, such as ion exchange on resins,¹ reverse osmosis,² and desalination.^{3,4} Most of the conventional separation and concentration processes used in hydrometallurgy, such as precipitation, ion exchange on resins, ore

leaching or liquid–liquid extraction, are currently being reconsidered for their potential replacement by processes using synthetic membranes. Membrane separation techniques have drawn worldwide attention, and they are gradually used in industry. Membranes have been considered and formulated to accomplish a high level of efficiency and selectivity, while maintaining high mechanical strength and contamination resistance at low processing costs.⁵ Polymer inclusion membranes (PIMs) have been used for the extraction of numerous anionic and cationic

inorganic compounds,⁶ and small organic molecules.⁷⁻⁹ After mixing the base polymer, carrier, and plasticizer with a suitable solvent, the membrane matrix is obtained through a slow solvent evaporation process. The resulting polymer inclusion membrane is thin, flexible and forms a film.¹⁰ The base polymer used is very important in terms of the mechanical strength of the membrane.

In order to recycle and reuse wastewater, one of the solutions that seem very promising is the implementation of membrane filtration systems capable of ensuring the disinfection of effluents. These systems often use organic membranes based on several polymers.^{11,12} Cellulose triacetate (CTA) is a basic polymer commonly used in the preparation of polymer inclusion membranes (PIMs). CTA is a polar polymer, with a number of acetyl and hydroxyl moieties that are capable of forming highly oriented hydrogen bonding, giving CTA a crystalline structure.¹³ CTA membranes can be tailored for a wide range of permeability and flux performance. CTA-based materials are widely used in membrane technology because they are not prone to fouling. Thus, their porosity and water permeability increase over time, which helps preserve their long-term performance. Sugiura *et al.* were the first researchers who prepared polymer inclusion membranes using cellulose triacetate as the basic polymer.¹⁴⁻¹⁶ PIMs have been efficaciously used in some application areas, such as biochemistry, agronomy, chemistry, medicine, pharmaceuticals, water treatment and fine chemical separations, principally in nuclear industry.¹⁷⁻²⁰ The selective separation of this kind of polymeric membranes is accomplished frequently by the presence of selective compounds, called carriers, in the membrane phase. Recently, our research group combined polymer inclusion membranes (PIMs) with semiconductors to improve the performance of metal ions transfer.²¹⁻³⁶ It should be noted that the plasticizer acts as a binder between the different components of the membrane, giving the membrane greater flexibility. Furthermore, the addition of clay or nanoparticles improves the hydrophilic character of the membrane and greatly increases the retention of metallic ions by adsorption.

This work focuses on the preparation and characterization of hybrid membranes by incorporating Algerian kaolin into the polymer solution of cellulose triacetate and a plasticizer using the phase inversion technique. The

objective of this work is the valorization of a local clay, namely kaolin, by its incorporation into polymeric membranes designed for the treatment of water polluted by inorganic contaminants – heavy metals (lead and cadmium) – by both filtration and adsorption. Various characterization techniques, including scanning electron microscopy (SEM), Fourier-transform infrared spectroscopy (FTIR) and thermogravimetric analysis (TGA), were employed to evaluate the properties of the obtained hybrid membranes. The synthesized membranes were applied to treat a synthetic aqueous solution contaminated with heavy metals, namely lead (Pb^{2+}) and cadmium (Cd^{2+}) ions. The results demonstrated significant changes in the structural and performance characteristics of the membranes due to the addition of the adsorbent.

EXPERIMENTAL

Materials

All reagents were used as received, without any further purification. CTA (pure) and chloroform (GC $\geq 99\%$) were purchased from Fluka. Dioctyle phthalate (DOP), lead nitrates $\text{Pb}(\text{NO}_3)_2$ and cadmium nitrates $\text{Cd}(\text{NO}_3)_2$ were obtained from Carlo Erba. The clay (kaolin), used as a solid support was Algerian kaolinite extracted from Roussel in Jijel (Algeria). It was supplied by ENOF Chemical Ltd. Research Company for Non-Ferrous Matters, Algeria. The aqueous solutions containing heavy metals were prepared by dissolving the different reagents ($\text{Pb}(\text{NO}_3)_2$ and $\text{Cd}(\text{NO}_3)_2$) in deionized water.

Membrane preparation method

The membranes were prepared via phase inversion. In this method, CTA and kaolin were dissolved in CHCl_3 . Then, the plasticizer DOP was added under vigorous stirring for 3 hours (Fig. 1). The solution was then transferred into a circular glass container and degassed in an ultrasonic cleaner for 15 min to remove air bubbles to form a homogeneous and stable solution. After degassing, the casting solution was left for slow evaporation for 24 hours. The resulting membrane was extracted by the addition of distilled water. The membrane consists of 0.4 g of CTA and 0.2 mL of DOP, the average thickness of membrane is 90 μm , and specific surface area is 9.6 cm^2 , whereas the electrical resistance of the elaborated membrane is 5.2 $\text{k}\Omega$ when in contact with pure water at pH ~ 7 .

It is important to note that for the development of the membranes, we used three methods: in the first case, kaolin was mixed directly with CTA at different percentages of the adsorbent (5%, 7% or 9%), then, the plasticizer DOP was added to the homogeneous solution containing CTA and kaolin. The second possibility was to add kaolin to the homogeneous

solution containing (CTA and DOP). The last possibility was to use a mixture of CTA, DOP and kaolin in the same solution. The different combinations between the polymer (CTA), plasticizer (DOP), and

kaolin used for the preparation of the different membranes are reported in Table 1.

Table 1
Compositions of all synthesized polymeric membranes

Polymeric membranes	CTA (g)	DOP (mL)	Kaolin (g)
M1 (65%CTA + 30%DOP) + 5% Kaolin	0.4	0.2	0.0363
M2 (65%CTA + 5% Kaolin) + 30%DOP	0.4	0.2	0.0363
M3 65%CTA + 30%DOP + 5% Kaolin	0.4	0.2	0.0363
M4 (63%CTA + 7% Kaolin) + 30%DOP	0.4	0.2	0.0452
M5 (61%CTA + 9% Kaolin) + 30%DOP	0.4	0.2	0.0600

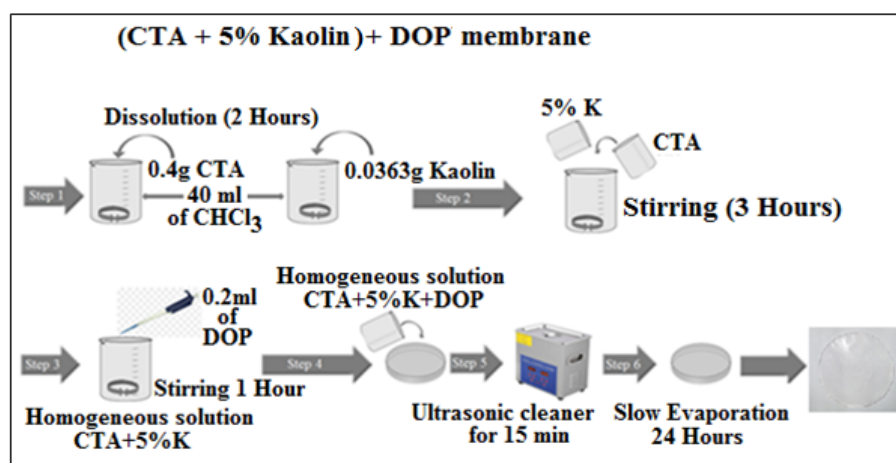


Figure 1: Preparation procedure of nanocomposite membranes

Characterization techniques

FTIR spectroscopy was used to observe the frequency changes of the functional groups. This technique was used to detect the presence of the different bonds of constituents used in the initial mixture and final polymeric membranes. The FTIR spectra were recorded with a Perkin-Elmer spectrometer (Spectrum One) (Perkin-Elmer Company, USA). The instrument was calibrated before analysis using 60 scans at a resolution of 2 cm^{-1} in the wavenumber range of $4000\text{--}400\text{ cm}^{-1}$.

Qualitative characteristics (dense or porous membranes) and quantitative characteristics, such as porosity and layer thickness, can be easily determined by SEM. The morphologies of the different membranes were determined by SEM analysis using a JEOL JSM 6301F FEG (JEOL Company, USA), with a voltage of 20 KV. Each sample was covered with platinum after being desiccated in a vacuum oven at low temperature.

Thermogravimetric analysis is considered a simple and suitable method to evaluate the thermal stability of different materials. TGA allows observing the effects of thermal decomposition, evaporation, reduction, desorption, sublimation, oxidation and absorption. TGA analyses were realized using a TGA Q500, (TA

Instrument Company, USA), automated from 50 to 600 °C at a rate of 10 °C/min . All samples were purged with nitrogen gas at a flow rate of 60 mL/min . The sample weights were approximately 10 mg.

The metal concentration was determined by sampling, at different time intervals, aliquots (0.5 mL) from both the feed and strip solutions, which were analyzed using the atomic absorption spectroscopy technique (AAS) with a Perkin-Elmer AAnalyst 700 model (Perkin-Elmer Company, USA) for Pb^{2+} and Cd^{2+} .

Transport experiments

The cell used for transport experiments consisted of two compartments, made of Teflon, with a maximum filling volume of 100 mL, separated by the polymeric membrane (Fig. 2). The feed compartment contained the metal solution at a concentration of 50 ppm of metal salt ($\text{pH} \sim 6$). The strip compartment contained distilled water. Both the feed and strip aqueous phases were stirred at 800 rpm using a magnetic stirrer. The membrane surface area was 9.61 cm^2 . Three independent experiments were realized to determine the metal ion concentration. The experimental standard deviation was determined to be $\pm 5\%$.

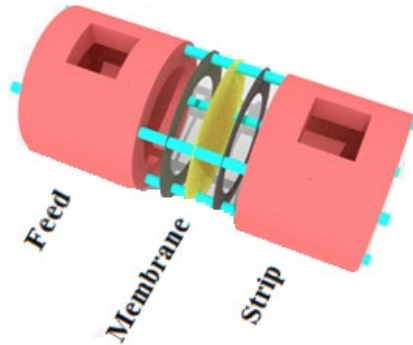


Figure 2: Dialysis cell scheme

RESULTS AND DISCUSSION

FTIR characterization

Figure 3 shows the spectra of the CTA membrane plasticized by DOP and modified by the incorporation of 5% of Algerian kaolin in comparison with the spectra of CTA and kaolin.

The main feature of the spectrum of kaolin is an absorption band located around 936 cm^{-1} , attributed to the angular deformation of the Si–O–Al group. The band at 651 cm^{-1} corresponds to the stretching mode of (Si–O) single bonds. The same figure also shows the presence of Al–O bands detected at 450 cm^{-1} . The FTIR spectrum of CTA shows a band at 2947 cm^{-1} attributed to elongation vibrations of the asymmetric C–H bonds and a band at 2875 cm^{-1} characteristic of symmetric ones. The presence of carbonyl groups of the ester function was evidenced by the existence of a band located at around 1732 cm^{-1} . We also noted that the CTA absorbed at around 1166 and 1048 cm^{-1} , corresponding to the

asymmetric and symmetric elongation vibrations of (C–O–C) groups.

The obtained results showed that all the maximum values observed in the spectrum of the CTA reference membrane, *i.e.* without plasticizer and kaolin, are present in the spectra of the modified membranes, in addition to those of the clay molecules that also involve the radicals detected in the $1000\text{--}400\text{ cm}^{-1}$ region. The main features of these spectra are an absorption band located around 1732 cm^{-1} , which is attributed to stretching vibrations of the carbonyl group of the CTA polymer. The bands at $1228\text{--}1232$ and 1035 cm^{-1} correspond to the asymmetric and symmetric stretching modes of C–O–C single bonds, respectively. The less intense bands at 2947 and 2880 cm^{-1} are attributed to C–H bonds and the wide band detected in the $3500\text{--}3300\text{ cm}^{-1}$ region is attributed to the O–H bond stretching modes of the CTA polymer.

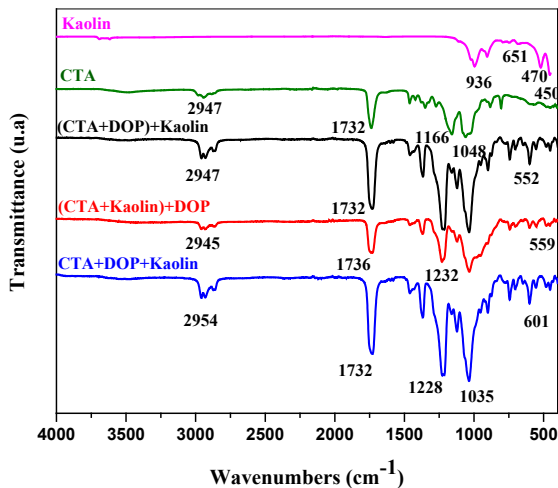


Figure 3: FTIR spectra of the synthesized membranes compared to those of CTA and kaolin

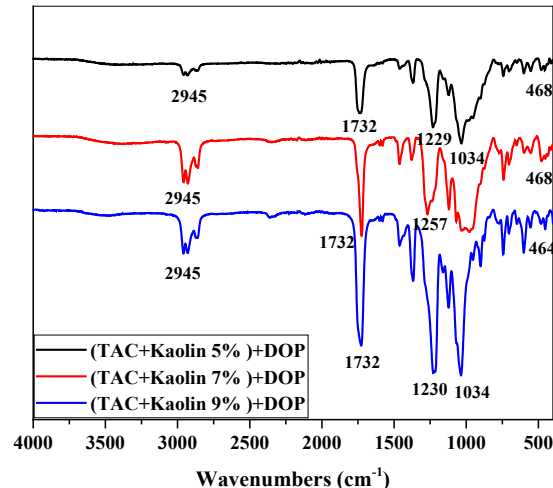


Figure 4: FTIR spectra of the synthesized membranes with different clay percentage

We also noted a decrease in the intensity of the 2962 and 2877 cm^{-1} bands and the displacement

of the band at 1225 cm^{-1} toward larger wavenumbers (1232 cm^{-1}). Four other bands

confirming the presence of the kaolin were detected in the same figure characteristic of the presence of Fe_2O_3 bonds detected at 470 cm^{-1} . The wide band at 450 cm^{-1} is due to Al–O bonds and an absorption band located around 936 cm^{-1} is attributed to the angular deformation of the Si–O–Al group. The band observed at about $552\text{--}651\text{ cm}^{-1}$ is attributed to the vibration of Si–O bands.

Ultimately, the results obtained show that the interconnected chains of the polymer with the plasticizer and kaolin are independent of the preparation method.

The FTIR spectra of the elaborated membranes using 5%, 7% and 9% of kaolin are illustrated in Figure 4. As can be seen, it is rather difficult to discern any difference among them. Nevertheless, the presence of all the functional groups of the different constituents (polymers, plasticizer, and kaolin) is noted for each

membrane.

Thermal analysis

Figures 5–7 show the thermal behaviors of the membranes prepared in this study by different elaboration methods. All the membranes exhibited thermal stability until $180\text{ }^\circ\text{C}$. Their thermal degradation occurs in two main steps. During the first one, which occurred over a temperature range of $150\text{--}250\text{ }^\circ\text{C}$, the membrane lost about 31–42 wt% of its initial mass, with a T_{max} at about $243\text{--}258\text{ }^\circ\text{C}$. This important weight loss is probably due to the degradation of the plasticizer DOP. In the second stage of degradation of the membrane, which occurred between 300 and $380\text{ }^\circ\text{C}$, a weight loss of about 50–56 wt% was recorded, with T_{max} at $350\text{ }^\circ\text{C}$. This stage is attributed to the degradation of CTA polymeric chains.

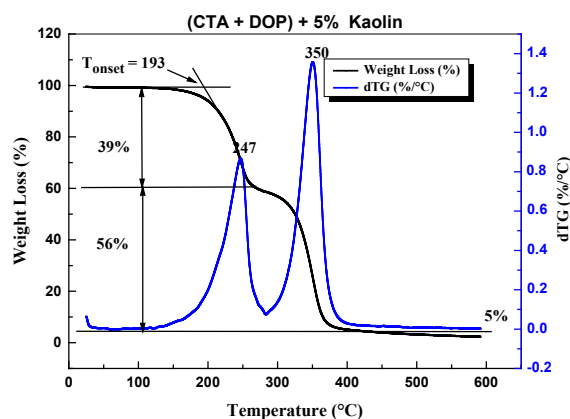


Figure 5: Thermogravimetric (TGA and dTG) curves of the synthesized membrane (CTA + DOP) + 5% Kaolin

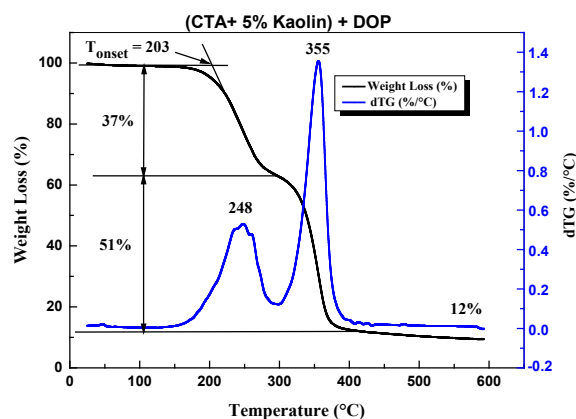


Figure 6: Thermogravimetric (TGA and dTG) curves of the synthesized membrane (CTA + 5% Kaolin) + DOP

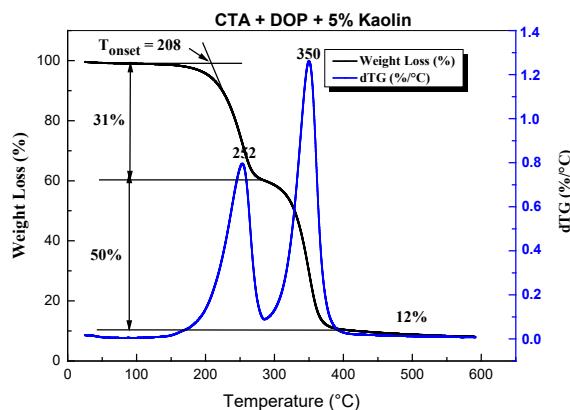


Figure 7: Thermogravimetric (TGA and dTG) curves of the synthesized membrane (CTA + DOP + 5% Kaolin)

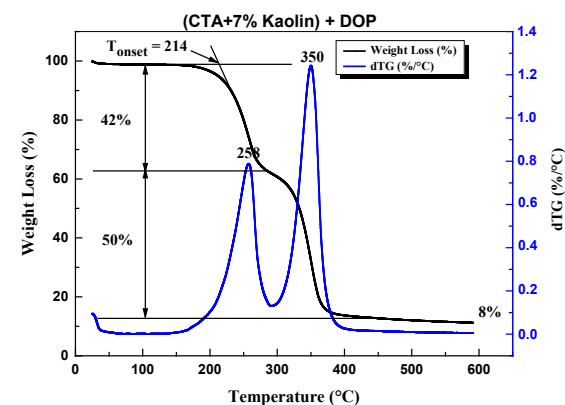


Figure 8: Thermogravimetric (TGA and dTG) curves of the synthesized membrane (CTA + 7% Kaolin) + DOP

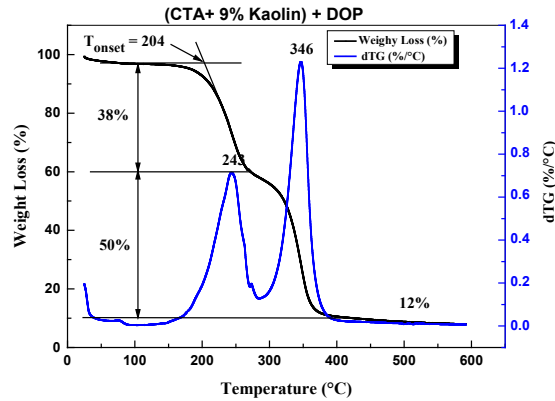


Figure 9: Thermogravimetric (TGA and dTG) curves of the synthesized membrane (CTA+ 9% Kaolin) + DOP

The TGA and dTGA thermograms of the (63% CTA + 30% DOP + 7% Kaolin) and (61% CTA + 30% DOP + 9% Kaolin) membranes, shown in Figures 8 and 9, respectively, illustrate that the process of degradation of these two membranes occurred into two main stages. During the first one, in a temperature range 180–280 °C, the membrane lost about 38 to 42 wt% of its initial mass, with a T_{max} at 243 to 258 °C, and T_{onset} of 204 and 214 °C. A more important weight loss was recorded during the second stage of degradation (50 wt%), between 348 and 350 °C,

with a T_{max} at 350 °C. We note that the kaolin retards the degradation process, as shown by the shift of the thermogravimetric parameters to higher temperatures, when the kaolin was added to CTA and DOP plasticizer (T_{onset} of 214 °C for 7% and 203 °C for 5%).

The thermogravimetric parameters recorded for the synthesized membranes are summarized in Table 2. Finally, the TGA results obtained show clearly that all synthesized membranes exhibited good thermal stability, which was independent of the elaboration method.

Table 2
Values of some thermogravimetric parameters of the synthesized membranes

Membrane	T_{onset} (°C)	T_{max} (°C)	Weight loss (wt%)	Residue (%)
M1 (CTA + DOP) + 5% Kaolin	193	247 350	39 56	05
M2 (CTA + 5% Kaolin) + DOP	203	248 355	37 51	12
M3 CTA + DOP + 5% Kaolin	208	252 350	38 50	12
M4 (CTA + 7% Kaolin) + DOP	214	258 350	42 50	08
M5 (CTA + 9% Kaolin) + DOP	204	243 346	38 50	12

Contact angle measurements

A comparison of the hydrophobicity of the synthesized composite membranes by measuring their water contact angles is shown in Table 3. Compared with the CTA + DOP + Kaolin control membrane ($60.0^\circ \pm 0.2^\circ$), the water contact angles of the composite membranes were found to decrease noticeably (55.5° and 53.1°), when the quantities of clay increase (7% and 9%),

respectively. Lower water contact angles correspond to more hydrophilic surfaces. The improved hydrophilicity of the synthesized composite membranes can be attributed to the presence of hydrophilic clay, arising from the hydroxyl functional groups on its surface. At the same time, a decrease in the average contact angles indicates successful incorporation of the clay into the polymer matrix.

Table 3
Contact angles of all synthesized membranes

Membrane	Contact angle (°)
M1 (65%CTA + 30%DOP) + 5%K	61.59 ± 0.2
M2 (65%CTA + 5% K) + 30%DOP	60.07 ± 0.2
M3 (65%CTA + 5% K + 30%DOP) in the same mixture	56.58 ± 0.2
M4 (63%CTA + 7%K) + 30%DOP	55.54 ± 0.2
M5 (61%CTA + 9%K) + 30%DOP	53.18 ± 0.2

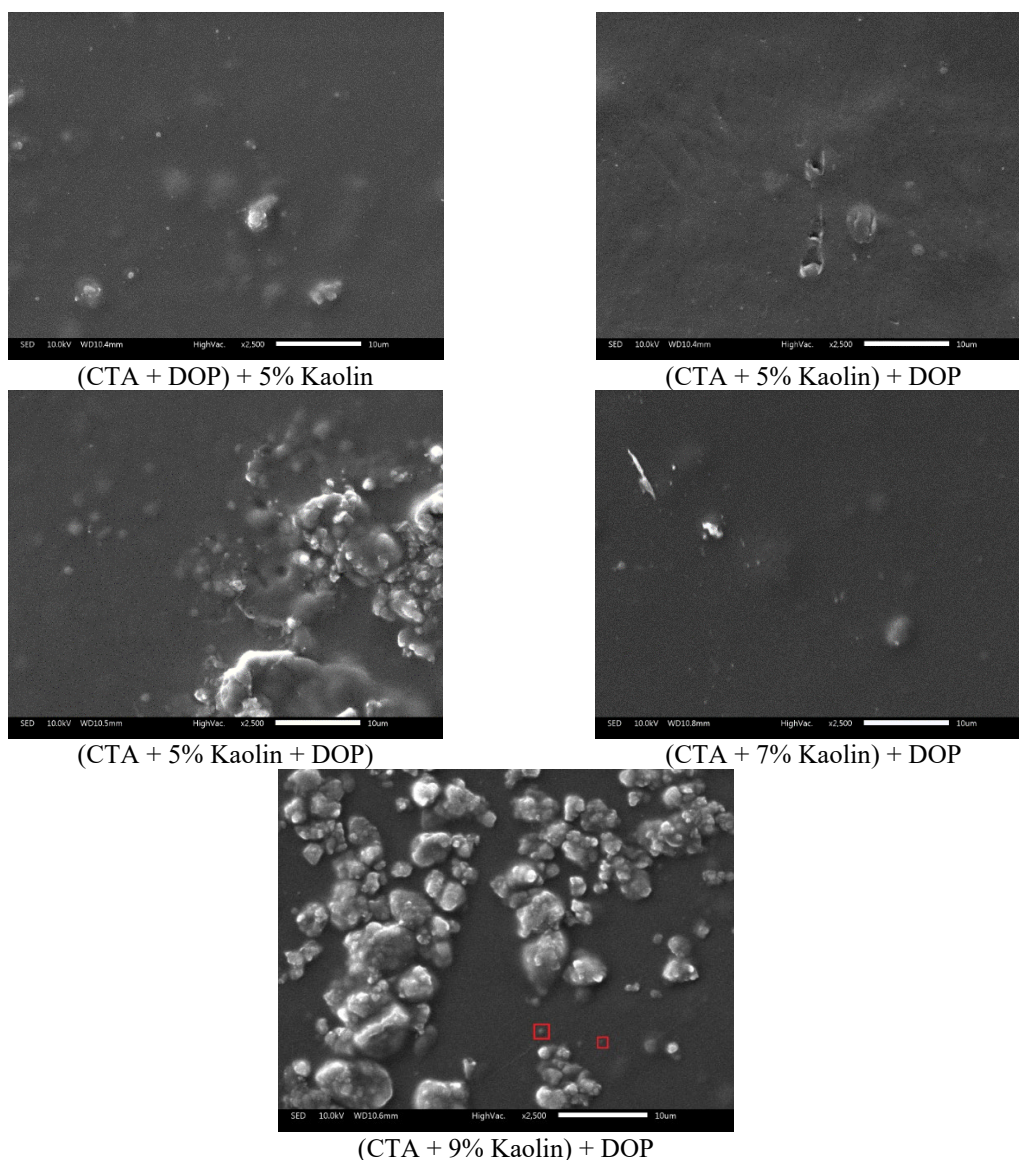


Figure 10: Scanning electron microscopy images of the synthesized composite membranes

SEM characterization

One important aspect of PIMs is the microstructure of the membrane materials, which determines the distribution of the kaolin in the polymer matrix and ultimately affects the membrane transport efficiency. Figure 10 shows the morphology of the differently prepared membranes.

Surface images of hybrid membranes reveal no visible pores, and a smooth dense surface. Nanoparticles ranging from 200 to 500 nm in size are clearly observed over the membrane surface. However, the surface morphology became much rougher in the case of the incorporation of 9% of clay, compared to that of the nanocomposite membrane filled with 5% of clay, which

potentially increases the membrane surface area and thereby enhances the water flux. The FTIR spectra showed the presence of silica bands, which are characteristic of clay, thus confirming the presence of clay in the membrane.

Application of elaborated membranes for water purification

Figure 11 presents the percentage of retention of Pb^{2+} and Cd^{2+} fixed in the membrane. The initial concentration of the metallic ions in the feed phase was fixed to 50 ppm. The transport has been achieved using the five membranes prepared in this work, containing CTA, DOP and Kaolin. This figure shows clearly that the retention of lead is significantly higher than that of cadmium using all synthesized composite membranes. We clearly see that membrane 4 (CTA + 7% Kaolin) + DOP proved a good performance by fixing 56.8% of

lead. This result confirms the affinity between the components of the membranes (polymer, plasticizer and inorganic adsorbent agent) towards the metallic ions (Pb^{2+}) and proves that the addition of the clay (kaolin) facilitated the fixation of lead ions. This result confirms also that the best method to synthesize this kind of composite membranes is to mix the polymer with clay in the first stage, and after that, to add the plasticizer. It is important to note that the adsorption of Pb (II) and Cd (II) ions onto kaolinite clay decreased with increasing percentage of the adsorbent (7% to 9%). The surface of the kaolinite clay sample contains some active sites, which may become positively charged by the fixation of Pb^{2+} and Cd^{2+} . This increases the competition between H^+ and the metal ions for available adsorption sites. This result is in accordance with the literature.^{37,38}

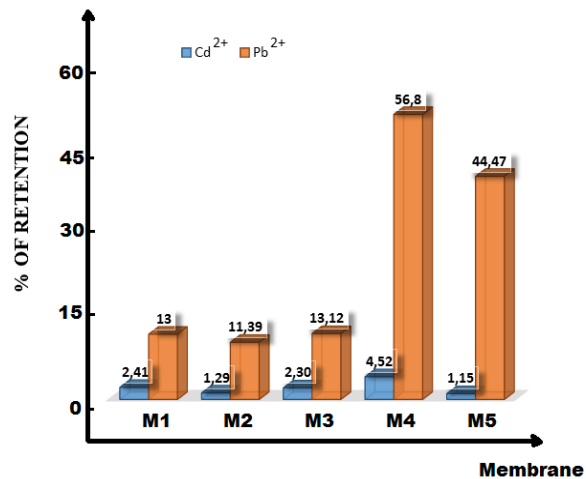


Figure 11: Percentage of retention of lead and cadmium ions onto all synthesized composite membranes

CONCLUSION

This study presents the polymer–clay combination as a powerful sorption material for water purification from inorganic contaminants both by filtration and by adsorption. A novel composite membrane was synthesized using a mixture of polymer, plasticizer and Algerian clay. Composites membranes were successfully elaborated by solution casting, followed by solvent evaporation using cellulose triacetate as polymer matrix. All the synthesized membranes were characterized by physical methods, like Fourier transform infrared spectroscopy, thermal analysis, scanning electron microscopy and contact angle measurement. FTIR spectroscopy confirmed the coexistence of all the components of each membrane. The degradation of the

membranes occurred via a two-step process, with the main loss starting at 190 °C, due to the thermal degradation of the plasticizer. This result confirmed that all the synthesized membranes exhibited good thermal stability. The SEM observation of the membranes revealed a dense and homogeneous structure. The kaolin promotes the membrane hydrophilicity, decreasing the contact angle. It was also concluded that the combination of clay and polymeric membrane is very efficient to eliminate heavy metals and increase considerably their rejection. Finally, the polymer–clay combination was found to be most economical, and total elimination of heavy metals can be obtained after two or three cycles of purification.

REFERENCES

- ¹ D. Y. Takigawa, *Separ. Sci. Technol.*, **27**, 325 (1992), <https://doi.org/10.1080/01496399208018883>
- ² D. Akretche, A. Gherrou and H. Kerdjoudj, *Hydrometallurgy*, **46**, 287, (1997), [https://doi.org/10.1016/S0304-386X\(97\)00026-1](https://doi.org/10.1016/S0304-386X(97)00026-1)
- ³ R. W. Matthews, *J. Catal.*, **111**, 264 (1988), [https://doi.org/10.1016/0021-9517\(88\)90085-1](https://doi.org/10.1016/0021-9517(88)90085-1)
- ⁴ A. Troupis, E. Grika, A. Hiskia and E. Papaconstantinou, *C. R. Chim.*, **9**, 851 (2006), <https://doi.org/10.1016/j.crci.2005.02.041>
- ⁵ P. S. Goh, T. Matsuura, A. F. Ismail and N. Hilal, *Desalination*, **391**, 43 (2016), <https://doi.org/10.1016/j.desal.2015.12.016>
- ⁶ M. Safarpour, A. Safikhani and V. Vatanpour, *Separ. Purif. Technol.*, **279**, 119678 (2021), <https://doi.org/10.1016/j.seppur.2021.119678>
- ⁷ E. Anticó, R. Vera, F. Vázquez, C. Fontàs, C. Lu *et al.*, *Materials*, **14**, 15 (2021), <https://doi.org/10.3390/ma14040878>
- ⁸ M. I. G. S. Almeida, R. W. Cattrall and S. D. Kolev, *J. Membr. Sci.*, **415–416**, 9 (2012), <https://doi.org/10.1016/j.memsci.2012.06.006>
- ⁹ M. I. G. S. Almeida, R. W. Cattrall and S. D. Kolev, *Anal. Chim. Acta*, **987**, 14 (2017), <https://doi.org/10.1016/j.aca.2017.07.032>
- ¹⁰ A. Kaya, C. Onac and H. K. Alpoguz, *J. Hazard. Mater.*, **317**, 1 (2016), <https://doi.org/10.1016/j.jhazmat.2016.05.047>
- ¹¹ P. J. James, T. J. McMaster, J. M. Newton and M. J. Miles, *Polymer*, **41**, 4223 (2000), [https://doi.org/10.1016/S0032-3861\(99\)00641-2](https://doi.org/10.1016/S0032-3861(99)00641-2)
- ¹² N. Abdellaoui-Arous, A. S. Hadj-Hamou and S. Djadoun, *Thermochim. Acta*, **547**, 22 (2012), <https://doi.org/10.1016/j.tca.2012.08.015>
- ¹³ L. D. Nghiem, P. Mornane and I. D. Potter, *J. Membr. Sci.*, **281**, 7 (2006), <https://doi.org/10.1016/j.memsci.2006.03.035>
- ¹⁴ M. Sugiura, M. Kikkawa and S. Urita, *Separ. Sci. Technol.*, **22**, 2263 (1987), <https://doi.org/10.1080/01496398708068612>
- ¹⁵ M. Sugiura, M. Kikkawa and S. Urita, *J. Membr. Sci.*, **42**, 47 (1989), [https://doi.org/10.1016/S0376-7388\(00\)82364-9](https://doi.org/10.1016/S0376-7388(00)82364-9)
- ¹⁶ M. Sugiura, *Separ. Sci. Technol.*, **28**, 1453 (1993), <https://doi.org/10.1080/01496399308018050>
- ¹⁷ O. Arous, A. Gherrou and H. Kerdjoudj, *Separ. Sci. Technol.*, **39**, 1681 (2004), <https://doi.org/10.1081/SS-120030792>
- ¹⁸ H. Inoue, M. Kagoshima, M. Yamasaki and Y. Honda, *Appl. Radiat. Isot.*, **61**, 1189 (2004), <https://doi.org/10.1016/j.apradiso.2004.04.014>
- ¹⁹ K. Maiphethlo, L. Chimuka, H. Tutu and H. Richards, *Sci. Total Environ.*, **799**, 149483 (2021), <https://doi.org/10.1016/j.scitotenv.2021.149483>
- ²⁰ D. Bożejewicz, K. Witt and M. A. Kaczorowska, *Desal. Water Treat.*, **214**, 194 (2021), <https://doi.org/10.5004/dwt.2021.26659>
- ²¹ D. Berdous, N. Abdellaoui, O. Arous and D. E. Akretche, *Macromol. Symp.*, **408**, 2200066 (2023), <https://doi.org/10.1002/masy.202200066>
- ²² N. Draï, N. Abdellaoui, F. Saïb, O. Arous and M. Trari, *Desal. Water Treat.*, **255**, 185 (2022), <https://doi.org/10.5004/dwt.2022.28340>
- ²³ A. Yahia Cherif, O. Arous, M. Amara, S. Omeiri, H. Kerdjoudj *et al.*, *J. Hazard. Mater.*, **227**, 386 (2012), <https://doi.org/10.1016/j.jhazmat.2012.05.076>
- ²⁴ S. Bensaadi, N. Nasrallah, A. Amrane, M. Trari, H. Kerdjoudj *et al.*, *J. Env. Chem. Eng.*, **5**, 1037 (2017), <https://doi.org/10.1016/j.jece.2017.01.014>
- ²⁵ F. Saïb, O. Arous, A. Mazari and M. Trari, *Macromol. Symp.*, **386**, 1 (2019), <https://doi.org/10.1002/masy.201800245>
- ²⁶ K. Agoudjil, N. Haddadine, N. Bouslah, O. Arous, F. Saïb *et al.*, *Cellulose Chem. Technol.*, **57**, 617 (2023), <https://doi.org/10.35812/CelluloseChemTechnol.2023.57.56>
- ²⁷ H. Briki, N. Abdellaoui, O. Arous, F. Metref and D. E. Akretche, *Cellulose Chem. Technol.*, **56**, 1109 (2022), <https://doi.org/10.35812/CelluloseChemTechnol.2022.56.99>
- ²⁸ N. Abdellaoui and O. Arous, *Macromol. Symp.*, **386**, 1800244 (2019), <https://doi.org/10.1002/masy.201800244>
- ²⁹ N. Abdellaoui, Z. Himeur and O. Arous, *Macromol. Symp.*, **386**, 1800240 (2019), <https://doi.org/10.1002/masy.201800240>
- ³⁰ N. Abdellaoui, F. M. Laoui, H. Cerbah and O. Arous, *J. Appl. Polym. Sci.*, **135**, 46592 (2018), <https://doi.org/10.1002/app.46592>
- ³¹ D. Hamane, O. Arous, F. Kaouah, M. Trari, H. Kerdjoudj *et al.*, *J. Env. Chem. Eng.*, **3**, 60 (2015), <https://doi.org/10.1016/j.jece.2014.11.003>
- ³² L. D. Nghiem, P. Mornane, I. D. Potter, J. M. Perera and R. W. Cattrall, *J. Membr. Sci.*, **281**, 7 (2006), <https://doi.org/10.1016/j.memsci.2006.03.035>
- ³³ M. Ulewicz, U. Lesinska, M. Bochenska and W. Walkowiak, *Separ. Sci. Technol.*, **54**, 299 (2007), <https://doi.org/10.1016/j.seppur.2006.09.018>
- ³⁴ E. Radzaminska-Lenarcik, I. Pyszka and M. Ulewicz, *Membranes*, **10**, 88 (2020), <https://doi.org/10.3390/membranes10050088>
- ³⁵ A. Ammi Said, O. Arous, A. Yahia Cherif, Y. Berbar, M. Amara *et al.*, *Polym. Bull.*, **76**, 3659, (2019), <https://doi.org/10.1007/s00289-018-2568-7>
- ³⁶ H. Briki, N. Abdellaoui, F. Metref, D. E. Akretche and O. Arous, *J. Biotech. Biores.*, **2**, 1 (2020), <https://doi.org/10.31031/JBB.2020.02.000539>
- ³⁷ K. Al-Essa and F. Khalili, *Am. J. Appl. Chem.*, **6**, 25 (2018), <https://doi.org/10.11648/j.ajac.20180601.14>
- ³⁸ Y. Zhang, L. Zang, Y. Zhao, Q. Wei and J. Han, *Toxics*, **11**, 961 (2023), <https://doi.org/10.3390/toxics.11120961>